

TECHNOLOGICAL PARAMETERS COMPARATIVELY STUDIED BY FEM AT CLASSIC AND ULTRASONIC AIDED MICROELECTRODISCHARGE MACHINING

Prof. Nicolae Ion MARINESCU¹, Assoc. Prof. Daniel GHICULESCU², SERGIU NANU³
DANIELA GHICULESCU⁴, GEORGE KAKARELIDIS⁵

¹“Politehnica” University of Bucharest, niculae.marinescu@nsn.pub.ro, ²“Politehnica” University of Bucharest, daniel.ghiculescu@nsn.pub.ro, ³“Politehnica” University of Bucharest, sergiu.nanu@nsn.pub.ro, ⁴National Authority for Scientific Research, daniela.ghiculescu@ancs.ro, Romania, ⁵Technological Educational Institute of Patras, gkakarel@gmail.com, Greece

Abstract: The paper deals with study through Finite Element Method (FEM) concerning the influence of technological parameters on material removal process at classic electrodischarge machining (EDM) finishing and micro(μ)EDM aided by ultrasonics (US). The working parameters used at μ EDM were analyzed in comparison with classic EDM ones, identifying some weaknesses of μ EDM. Different initial microgeometries were considered in order to study the material removal process. Some recommendations resulted from FEM aiming at improving some technological performances at EDM+US were formulated.

Keywords: ultrasonics, microelectrodischarge machining, technological parameters.

1. INTRODUCTION

The material removal process by micro-EDM offers some important opportunities in achievement of micro-components such as nozzle holes, slots, shafts and gears in any conductive material with a minimal conductivity of $k = 0.01$ S/cm including high temperature alloys, cemented carbide, and electro-conductive ceramics [1].

2. MICROEDM PARAMETERS AND SOLUTIONS FOR IMPROVEMENT

This up-to-date variant of the EDM process, micro-EDM, it is so called because it utilizes low discharge energies approximately in the range of $10^{-9} - 10^{-5}$ J to remove small volumes of material of around $0.05 - 500 \mu\text{m}^3$ [2]. Even a single discharge can be used.

The micro-EDM process features two very important disadvantages (fig.1). The first one is a rather slow machining process. The material removal rate is relative low comparing to other machining and micro-machining processes. This is due to low machining rate given by general conditions of EDM occurring, and especially to very narrow working gap (under $5 \mu\text{m}$), characteristic of μ EDM, leading to process instability. It is also a serial process (succesive discharge), while silicon fabrication processes for example, is parallel.

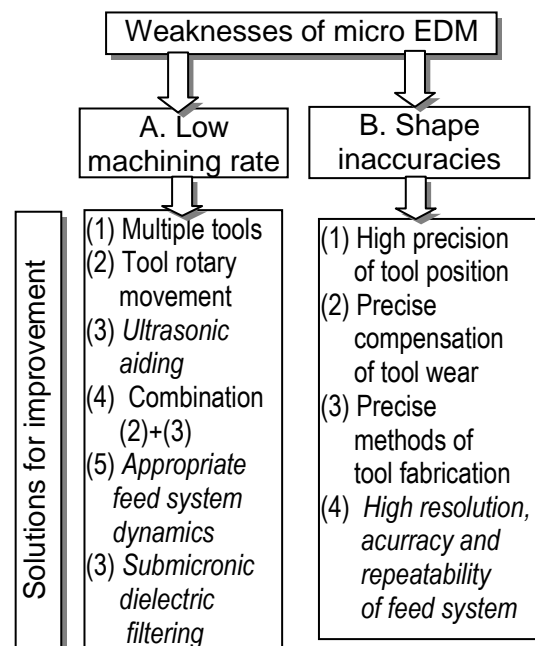


Fig. 1. Weaknesses of microEDM and solutions for improvement

Lithography and etching parallel nature makes them more productive [2].

The second weakness is high tool wear, leading to shape inaccuracies.

Several solutions to improve machining rate were undertaken (fig. 1). The solutions adopted by the authors were written in italics. A research direction was to drill multiple holes with multiple electrodes. In 1991, Higuchi et al. developed a pocket size EDM system [3]. Drilling one at a time instead hundreds or

thousands of holes was clearly inefficient. The pocket-sized EDM permits many the clamping systems to be placed on a large part, thus drilling several holes at the same time. More recently, other attempts to use multiple electrodes at microEDM were reported, obtaining a raise of machining rate [4], [5], [6]. However, the attempt to increase the number of electrode-tools working in parallel does not lead necessarily to proportional augment of machining rate due to increased number of short-circuits and consequently, corresponding retracts of electrode-tool. An optimum number of tools working in parallel to increase machining rate is needed to be found.

Other solutions could be indirect flusing produced by rotary movement of the electrode-tool. Ultrasonic aiding microEDM (μ EDM+US) is also included in this type of approach [1]. But μ EDM+US is more than that due to additional mechanism of material removal mechanism produced by ultrasonically induced cavitation. It reduces dramatically the gas bubble life around plasma channel at the most half-period of ultrasonic oscillations and consequently, could remove material in liquid state. Hydraulic material removal occurs too, determined by high pressure resulted from collective implosion of gas bubbles from the gap, which is of tens MPa order [7].

H. Huang at al. achieved spectacular increasing of machining rate up to 60 times at μ EDM+US of microholes in Nitinol, an intelligent material from Ni and Ti alloy, which keeps the shape after deformation and reheating [8]. J.C. hung at al. combined ultrasonic vibration with rotary movement of electrode-tool at microholes achieved by μ EDM [9].

Nevertheless ultrasonic aiding supposes additional costs to achieve the chains and the generator, which could be covered at higher volume of fabrication than at classic EDM.

The main methods for prevailing over shape inaccuracies introduced by tool wear are more precise position of the tool [10] or better compensation of tool wear [11]. Another approach to improve the accuracy of micro-EDM is to use more accurate method of tool fabrication like LIGA, an alternative microfabrication process combining deep X-ray lithography, plating-through-mask and molding. This enables the highly precise manufacture of high aspect ratio micro-

structures with large structural height ranging from hundreds to thousands of micrometers thickness, which are difficult to be achieved with other manufacturing techniques [12].

Several machines performing microEDM exist on the market today [2]. Most of them use RC circuits capable of producing pulses as short as 10 nano-seconds. It is obviously that using this type of pulse, very low discharge energy can be produced. On the other hand, relaxation pulses cannot be controlled in terms of delivery moment, which makes them unacceptable for US aiding - synchronization the current pulse with US oscillation stretching semiperiod [13]. The lowest values of static pulse durations, which are more suitable for US aiding, are 2.5 μ s in the state of the art. Then the value of 2 μ s used in our preliminary experiments is framed in requirements for microEDM; 0.9 A current is compatible with values provided by mentioned above installations [2].

Another key parameter addressing shape accuracy is feed system dynamics. This also affects the entire process, evaluated by machining rate, relative volumetric wear and surface roughness. All actual installations provide undermicrometer values for resolution and 1 μ m for position precision and repeatability. Our equipment is able to provide 0.5 μ m resolution and under 1 μ m for accuracy and repeatability being also compatible with the requirements.

The tool drawbacks affecting machining rate can be produced by high pollution of dielectric liquid from the gap. So, dielectric unit is also a very important element that has also an influence on accuracy if feed system has inappropriate dynamics. If a polluted dielectric with particles comparable with the gap size is provided, short-circuits can occur. Therefore it is recommended that μ EDM installation must be equipped with dielectric liquid unit with submicronic filtering capacity.

3. EXPERIMENTAL DATA

Reference experimental data considered for FEM modelling validation were synthesized in table 1, 2. These are obtained on a special equipment interfaced with Romanian ELER 01 machine, consisting in a new EDM generator for finishing and a feed system with 0.5 μ m resolution. For ultrasonic aiding we used 20 kHz frequency and 100 W consumed power on acoustic chain. The

crater diameters mean values were identified by photo-microscope Neophot – Zeiss with 500:1 magnifier. The crater depths were measured by surface roughness measurement apparatus, “Surtronic” Rank Taylor Hobson.

Table 1. Craters mean dimensions at classic EDM with and without US aiding

Machining	EDM		EDM+US	
	Depth [μm]	Radius [μm]	Depth [μm]	Radius [μm]
Crater dimensions	3.6	5.5	1.8	3.5
Workpiece material: X210Cr12; tool material: Cu 99.5; static pulse duration with pulse time $t=25\mu s$, pause time $t_0=12\mu s$, positive polarity, current step $I=0.9A$				

Table 2. Craters mean dimensions at microEDM with and without US aiding

Machining	EDM		EDM+US	
	Depth [μm]	Radius [μm]	Depth [μm]	Radius [μm]
Crater dimensions	2	3.7	1.6	3.2
Workpiece material: X210Cr12; tool material: Cu 99.5; static pulse duration with pulse time $t=2\mu s$, pause time $t_0=2\mu s$, positive polarity, current step $I=0.9A$				

In our preliminary μEDM experiments, 20 V discharge tension, 0.9 A discharge current and 2 μs static pulse duration (commanded pulse) were used. So the discharge energy resulted was around $1.2 \cdot 10^{-5}$ J, situated at superior part of required energy domain [2]. Using this discharge energy, the equipment will assure the appropriate current density to work under mm cross section of electrode-tool, assuring the stability of the process, according to [14] (table 3).

Table 3. Recommended current density (after Charmilles)

Tool material	Polarity	Workpiece material	Current density
Copper	+	Steel	15-25 A/cm ²

This is strongly related to US aiding; static pulse durations can be correlated with US oscillation in order to take advantage on collective implosion of bubbles from the gap. Working at superior range of microEDM [1], concerning cross section of electrode, seeks to cope with pressure developed by US cavitation. The US shock waves are directed along the working gap, contributing to surface quality and machining rate increasing.

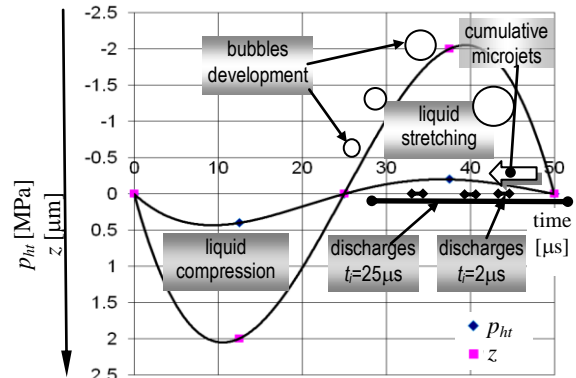


Fig. 2. Variation of total hydrostatic pressure (p_{ht}) along the tool elongation (z) in the frontal gap at $\mu EDM+US$

The total hydraulic pressure (p_{ht}), represented in fig. 2, together with elongation z of tool electrode which oscillates normally on machined surface, is determined by the relation:

$$p_{ht} = 2\pi \cdot c \cdot \rho \cdot f_{US} \cdot A \sin \omega t + p_h \quad [MPa] \quad (1)$$

where: c is sound velocity in dielectric liquid [m/s]; ρ - density of dielectric liquid [kg/m³]; f_{US} - ultrasonic frequency [Hz]; A - oscillation amplitude [m]; $\omega = 2\pi f_{US}$ [s⁻¹]; p_h - local hydraulic pressure from the gap [MPa]. The values from relation 2, corresponding to our real working conditions, under which cavitation was obtained, are: $\rho=840$ kg/m³; $c=(E/\rho)^{1/2}=(1.35 \times 10^9/840)^{1/2}=1267.7$ m/s; $f_{US}=20$ kHz, $A=2\mu m$; $p_h 0.1$ MPa.

At each final of stretching semiperiod (25 μs) after the gas bubbles from the gap grow, bubbles collective implosion is produced due due to p_{ht} increase at cumulative microjets stage - CMS, fig. 2. Huge pressure of tens MPa order is developed and shock waves parallel to machined surface decrease roughness by removing micropeaks with low shear resistance. The pulses of 25 μs and 2 μs are delivered as close as possible to CMS.

3. FINITE ELEMENT MODELLING

The new 4.2 version of Comsol Multiphysics was used in order to analyze comparatively the material removal mechanism by commanded pulses (static pulse duration) at classic finishing EDM and microEDM with and without ultrasonic aiding. The time dependent heat transfer module was used for modelling.

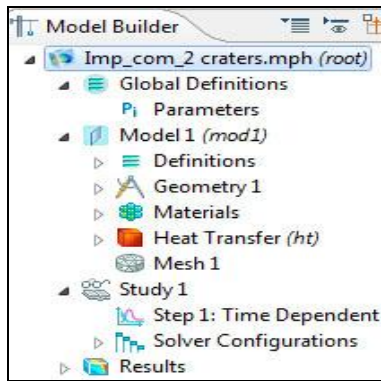


Fig. 3. Modelling stages in Comsol 4.2

The stages of FEM modelling are presented in fig. 3, representing the Model Builder.

In Global Definitions, the following parameters were considered in order to create a 2D geometry taking into account the symmetry of approached phenomena (fig. 4): lw =workpiece dimensions; ac =horizontal semiaxis and bc =vertical semiaxis of crater produced by previous discharge; rm = radius of profile formed by the resolidified material on crater margin (specific to static pulse duration); gb = radius of gas bubble formed around the plasma channel; workpiece dimensions of 10 mm was adopted after several studies; an optimum value was found aiming at calculation resources decrease and results precision increase.

Name	Expression	Value
lw	10[mm]	0.01 m
ac	3.5e-3[mm]	3.5E-6 m
bc	2e-3[mm]	2.0E-6 m
rm	0.1e-3[mm]	1.0E-7 m
gb	0.1[mm]	1.0E-4 m

Fig. 4. The parameters values for μ EDM modelling

An example of 2D geometry created for μ EDM with two previous craters is presented in fig. 5:

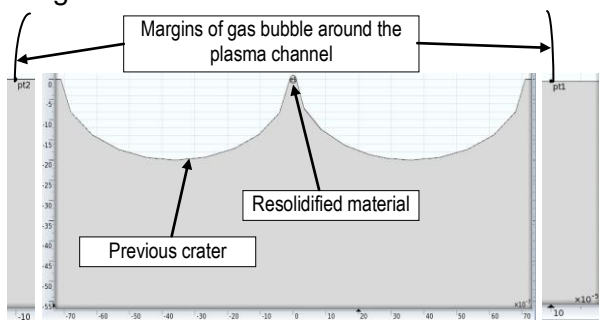
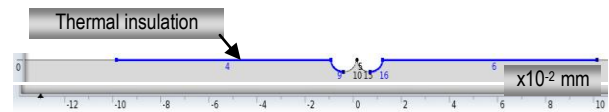


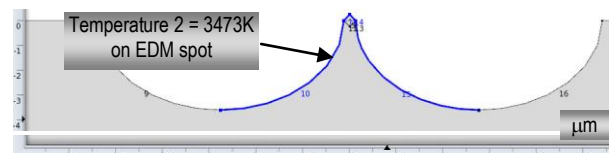
Fig. 5. 2D geometry for μ EDM

The machined material was D3 (UNS T30403), corresponding to X210Cr12 from Comsol library and completed with needed temperature dependent thermo-physical properties.

For boundary conditions, heat transfer in solids was used with the following restrictions: *Thermal insulation* in gas bubble zone (fig. 6-a); *Temperature 2 = 3473 K* on EDM spot (fig. 6-b); *Temperature 1 = 313.15 K*, on the rest of the surfaces with direct contact with dielectric liquid.



a) Thermal insulation in gas bubble zone



b) Temperature 2 = 3473 K on EDM spot

Fig. 6. Boundary conditions for pure EDM

The meshing was free triangular, finer in interest zone due to more vertex points of created geometry, which automatically takes into account the elements connectivity. The mesh medium quality was 9.68 on 1-10 scale, confirming appropriate results finally obtained. The statistical data of meshing are presented in fig. 7.

Statistics	
Complete mesh	
Element type:	All elements
Triangular elements:	2906
Edge elements:	231
Vertex elements:	14
– Domain element statistics –	
Number of elements:	2906
Minimum element quality:	0.7907
Average element quality:	0.9685
Element area ratio:	4.706E-8
Mesh area:	1.0E-4 m ²

Fig. 7. Statistical data of meshing

The temperature distribution obtained at classic EDM on two craters produced by previous discharges are presented in fig. 8. The crater dimensions are given by boiling isothermal disposal, based on Van Dijk's model of over heating [15].

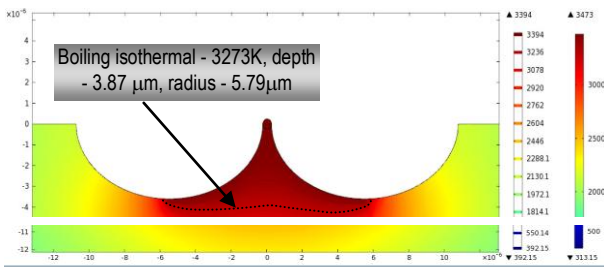


Fig. 8. Temperature distribution after 25µs commanded pulse at classic finishing EDM

This mechanism of material removal is based on temperature augment with 200-300 K over boiling point under normal conditions due to increased pressure during the pulse time on EDM spot. At pulse end, a sudden pressure decrease occurs, producing boiling of overheated material delimited by boiling isothermal.

In comparison, the volume removed by a single discharge at µEDM is more than four times smaller as it is presented in fig. 9.

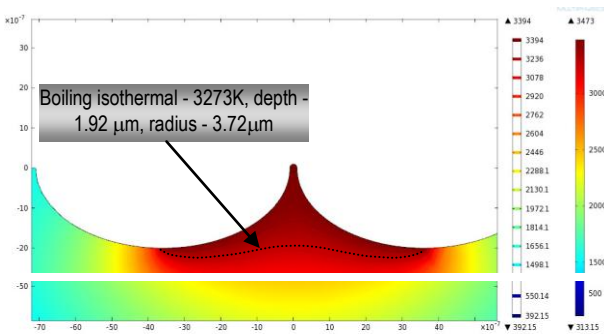


Fig. 9. Temperature distribution after 2µs commanded pulse at µEDM

The influence of initial geometries is essential on temperature distribution. Comparatively, the modelling starting from a plane surface produces craters with lower depth. An initial surface with four craters has the temperature distribution from fig. 10.

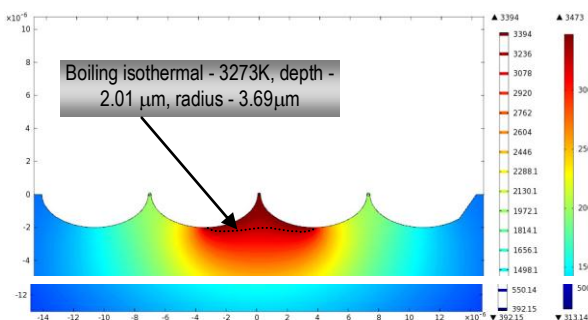


Fig. 10. Temperature distribution after 2µs commanded pulse at µEDM on initial four craters microgeometry

The initial four craters microgeometry affects the shape of the crater, increasing the depth and decreasing the radius (the depth/radius ratio increases). This is explained by the fact that discharge energy is dissipated on smaller volume adjacent to EDM spot, having a greater penetration on depth direction.

In case of classic EDM finishing, four craters initial microgeometry affects insignificantly the temperature distribution. This emphasizes that when modelling µEDM, in order to increase accuracy of results, it is necessary to create a microgeometry of initial surface as much as possible closer to real one in the zone neighboring the EDM spot.

Concerning the ultrasonic contribution to material removal mechanism, a possible synchronization between cumulative microjets stage and pulse duration disposal on time axis has to be analyzed (fig. 2).

The melted material by discharge is very fast resolidified. When working with 25 µs pulse time, less than 2 µs after pulse end is sufficient that temperature decreases under 1683 K, the solidification temperature of X210Cr12 (fig. 11). So, if cumulative microjets stage occurs after 2 µs from the pulse end, it cannot remove any melted material from the workpiece. This synchronization is very difficult to achieve because even a commanded pulse has a delay time when the breakdown of dielectric medium is accomplished.

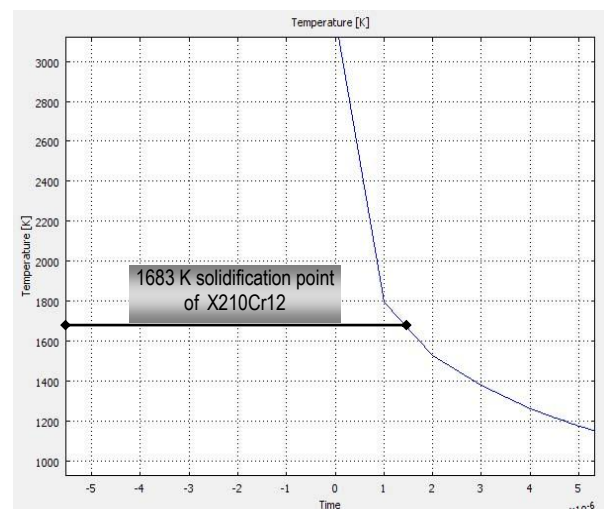


Fig. 11. Temperature evolution after 25µs pulse end at classic finishing EDM

A more realistic approach is to overlap the pulse duration on cumulative microjets stage (CMS).

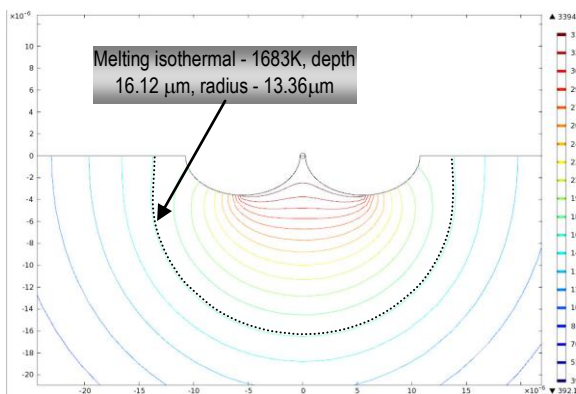


Fig. 12. Temperature distribution after 5 μ s from the beginning of commanded pulse at ultrasonic cumulative microjets stage

This is the case from fig. 12, when CMS occurs after 5 μ s from the beginning of the pulse. As one can see, taking into account the melting isothermal disposal, the potential of US material removal is very high. Thus the volume of removed material could be more than 2.5 times greater. This overlapping is more feasible at relative long durations of pulses, e.g. 25 μ s. At μ EDM+US, the additional mechanism of US removal consists mainly in crater margins removal (see table 1, 2) due to lower shear resistance against shock waves oriented parallel to machined surface [7].

4. CONCLUSIONS

Ultrasonic aiding microEDM with static pulse durations could be a solution to improve machining rate, precision and surface quality, appropriate for superior domain values of microholes, microslots, nozzle holes dimensions.

The initial microgeometry closer to real one in the zone adjacent to EDM spot is critical to increase the accuracy of the results at μ EDM modelling.

At μ EDM+US, the main additional ultrasonic mechanism of material removal is hydraulically break of microgeometry peaks contributing to machine roughness decrease and machining rate increase. Further researches will be focused on this phenomena modelling.

Acknowledgment: These paper results belong to CNMP Partnership project, 72-194.

REFERENCES

1. UHLMANN, E., REOHNER, M., LANGMACK, M. Micro EDM in Qin Yi,

Micromanufacturing Engineering and Technology, Elsevier 2010.

2. MOYLAN, S.P., CHANDRASEKAR, S., BENAVIDES, G. L., High-Speed Micro-Electro-Discharge Machining, Sandia National Laboratories, U.S. Department of Energy, Office of Scientific and Technical Information, 2005.

3. HUGUCHI, T., et al, Development of pocket-sized electro-discharge machine, Annals of the CIRP, vol. 40, p. 203-206, 1991.

4. TAKAHATA, K., GIANCHANDANI Y.B., Batch mode micro-EDM for high-density and high throughput micromachining, Proceedings of the IEEE: MEMS, p. 72-75. 2001.

5. TAKAHATA, K., GIANCHANDANI, Y.B. Batch mode micro-electro-discharge machining, Journal of MEMS, vol. 11 no. 2, p. 102-110. 2002.

6. WENG F.-T., HER, M.-G. Study of the batch production of micro parts using the EDM process, International Journal of Advanced Manufacturing Technology, vol. 19, p. 266-270., 2002.

7. Marinescu, N. I., Ghiculescu, D., Life duration of gas bubble formed around plasma channel at ultrasonic aided electrodischarge machining, Proceedings, The 20th DAAAM Symposium, p.0495-0496, Vienna, Austria.

8. HUANG, H. et al., Ultrasonic vibration assisted electro-discharge machining of microholes in Nitinol, J. Micromech. Microeng., 13 693-700, 2003.

9. HUNG, J.-C. et al., Using a helical micro-tool in micro-EDM combined with ultrasonic vibration for micro-hole machining, J. Micromech. Microeng., p. 2705-2713, Vol. 16, 2006.

10. YONG, L., et al., Research of micro electrodischarge machining equipment and process techniques, Chinese Journal of Mechanical Engineering, vol. 15 no. 2, pp 177-181, 2002.

11. WOLF, A., et al., Application of new actuator and vision control systems for micro electro discharge machining, Proceedings of the SPIE, p. 149-158, 1998.

12. TAKAHATA, K., et al., High-aspect-ratio WC-Co microstructure produced by the combination of LIGA and micro-EDM, Microsystem Technologies, vol. 6, p. 175-178, 2000.

13. GHICULESCU, D. et al., FEM study of synchronization between pulses and tool oscillations at ultrasonic aided micro-electrodischarge machining, Nonconventional technologies Review, no. 3, p. 19-25, 2010.

14. SÉMON, G. Guide pratique d'usinage par étincelage, Ateliers des Charmilles S.A., 1975.

15. VAN DIJCK, F., SNOEYS, R., Theoretical and Experimental Study of the Main Parameters Governing the Electrodischarge Machining Process, *Mecanique*, Vol. 301-302, p. 9-16. 1975.